

Direct visualization of atomically precise nitrogen-doped graphene nanoribbons

Cite as: Appl. Phys. Lett. **105**, 023101 (2014); <https://doi.org/10.1063/1.4884359>

Submitted: 05 May 2014 . Accepted: 09 June 2014 . Published Online: 14 July 2014

Yi Zhang, Yanfang Zhang, Geng Li, Jianchen Lu, Xiao Lin, Shixuan Du, Reinhard Berger, Xinliang Feng, Klaus Müllen, and Hong-Jun Gao



View Online



Export Citation



CrossMark

ARTICLES YOU MAY BE INTERESTED IN

[Bottom-up graphene nanoribbon field-effect transistors](#)

Applied Physics Letters **103**, 253114 (2013); <https://doi.org/10.1063/1.4855116>

[Graphene nanoribbon field-effect transistors fabricated by etchant-free transfer from Au\(788\)](#)

Applied Physics Letters **112**, 021602 (2018); <https://doi.org/10.1063/1.5006984>

[Construction of single-crystalline supramolecular networks of perchlorinated hexa-peri-hexabenzocoronene on Au\(111\)](#)

The Journal of Chemical Physics **142**, 101911 (2015); <https://doi.org/10.1063/1.4907369>



Your Qubits. Measured.

Meet the next generation of quantum analyzers

- Readout for up to 64 qubits
- Operation at up to 8.5 GHz, mixer-calibration-free
- Signal optimization with minimal latency

Find out more



Direct visualization of atomically precise nitrogen-doped graphene nanoribbons

Yi Zhang,¹ Yanfang Zhang,¹ Geng Li,¹ Jianchen Lu,¹ Xiao Lin,² Shixuan Du,^{1,a)} Reinhard Berger,³ Xinliang Feng,^{3,a)} Klaus Müllen,³ and Hong-Jun Gao¹

¹Institute of Physics and University of Chinese Academy of Sciences, Chinese Academy of Sciences, Beijing 100190, China

²University of Chinese Academy of Sciences and Institute of Physics, Chinese Academy of Sciences, Beijing 100049, China

³Max Planck Institute for Polymer Research, Ackermannweg 10, D-55128 Mainz, Germany

(Received 5 May 2014; accepted 9 June 2014; published online 14 July 2014)

We have fabricated atomically precise nitrogen-doped chevron-type graphene nanoribbons by using the on-surface synthesis technique combined with the nitrogen substitution of the precursors. Scanning tunneling microscopy and spectroscopy indicate that the well-defined nanoribbons tend to align with the neighbors side-by-side with a band gap of 1.02 eV, which is in good agreement with the density functional theory calculation result. The influence of the high precursor coverage on the quality of the nanoribbons is also studied. We find that graphene nanoribbons with sufficient aspect ratios can only be fabricated at sub-monolayer precursor coverage. This work provides a way to construct atomically precise nitrogen-doped graphene nanoribbons. © 2014 AIP Publishing LLC. [<http://dx.doi.org/10.1063/1.4884359>]

Graphene nanoribbons (GNRs), the quasi-one-dimensional strips of graphene with finite width (<10 nm) and high aspect ratios, have been considered as one of the most promising candidates for the future electronic devices due to their unique electronic and magnetic properties.^{1–3} Among these properties, the most fascinating one is the band gap opening at the Dirac point, which is strongly dependent on the lateral size and the edge geometry of the GNRs.^{4,5} Therefore, tuning the gap of GNRs has attracted tremendous attention.^{6–8} It has been reported that armchair GNRs (AGNRs) possess gaps inversely proportional to their width,⁵ and numerous efforts have been undertaken to fabricate AGNRs with different width, either by top-down^{6,8,9} or bottom-up approaches.^{10–12} Based on the on-surface reaction,^{13,14} the bottom-up approach shows the capability of controlling the width and edge structures. Moreover, the surfaces are almost contamination-free after the bottom-up synthesis processes and thus can be easily characterized by scanning tunneling microscopy and spectroscopy (STM/STS).^{10,15} Several kinds of AGNRs have been synthesized via specific molecular precursors, which were studied by STM and STS.^{11,12,16} Nevertheless, the width is restricted by the precursors and the ability to further tune the gap of AGNRs with certain width remains a big obstacle. Another promising way to modify the band gap is doping,^{17–20} while the precise control of the doping sites is still a challenging task so far. Taking the advantage of the bottom-up synthetic technique, precisely doped GNRs can be fabricated by introducing the heteroatoms into the oligophenylene precursors in advance. Recently, Bronner *et al.* have put this process into practice, and a shift of the band gap was observed by high-resolution electron energy loss spectroscopy (HREELS)

and photoelectron spectroscopy.²¹ However, direct imaging of the nitrogen-doped GNRs as well as the characterization of their electronic properties by STM and STS are still lacking.

In this Letter, we conduct a systematic study on the fabrication of nitrogen-doped chevron-type GNRs (NCGNRs) on Au(111), using rationally selected nitrogen substituted oligophenylene precursors. Combining STM experiments with the density functional theory (DFT) calculations, we confirm that NCGNRs have been fabricated. STS data show the band gap of the as-prepared NCGNRs is 1.02 eV, which are consistent with our theoretical calculations. The growth behaviors at both low coverage and high coverage are investigated. We find that high quality NCGNRs can only be obtained under sub-monolayer precursor coverage.

The experiments were performed under ultrahigh vacuum conditions, with a base pressure of 1×10^{-10} mbar. Atomically flat Au(111) surface was obtained by cycles of argon-ion sputtering and annealing to 470 °C. The precursor molecules were thermally evaporated at 180 °C onto the Au(111) surface, which was kept at room temperature. The samples were characterized by a commercial Omicron low temperature STM working at 78 K. All STM images are obtained in constant current mode and processed using Nanotec Electronica WSxM Scanning Probe Microscopy software.²² The possible geometrical structures and electronic properties are calculated using DFT based first principle calculations as implemented in Vienna *ab initio* simulation package (VASP).^{23,24} A $30 \text{ \AA} \times 30 \text{ \AA} \times 15 \text{ \AA}$ supercell and a $19 \text{ \AA} \times 30 \text{ \AA} \times 15 \text{ \AA}$ supercell are used for a free single molecule and the nanoribbons, respectively. Systematic tests demonstrated that the slabs are sufficient separated. The structures of NCGNRs are relaxed using the conjugated gradient method without any symmetric constraints. The electronic properties are calculated after full structural relaxation, using generalized gradient approximation (GGA) in the form proposed by Perdew, Burke, and Ernzerhof (PBE)²⁵ to express

^{a)}Authors to whom correspondence should be addressed. Electronic addresses: sxdu@iphy.ac.cn and feng@mpip-mainz.mpg.de. Tel.: +86-10-82649823 and +49-6131-379-488. Fax: +86-10-62556598 and +49-6131-379-100

the exchange-correlation energy of interaction among electrons, and the frozen-core projector augmented wave method is used to describe the interaction between ions and electrons.²⁶ The plane wave kinetic energy cutoff is 400 eV. The convergence criterion of the total energy is 10^{-4} eV, and the maximum residual force allowed on each atom is 0.01 eV/Å. The Brillouin zone is sampled by $(1 \times 1 \times 1)$ k points. The simulated STM images shown here are calculated using converged electronic densities within the Tersoff-Hamann approximation.²⁷

The typical bottom-up approach of fabricating GNRs is based on the Ullmann reaction, using aryl halides as the fundamental building blocks. Fig. 1 shows the basic NCGNRs fabrication approach with the 6,11-dibromo-1,4-diphenyl-2,3-dipyridyltriphenylene ($C_{40}Br_2N_2H_{24}$) molecule as the

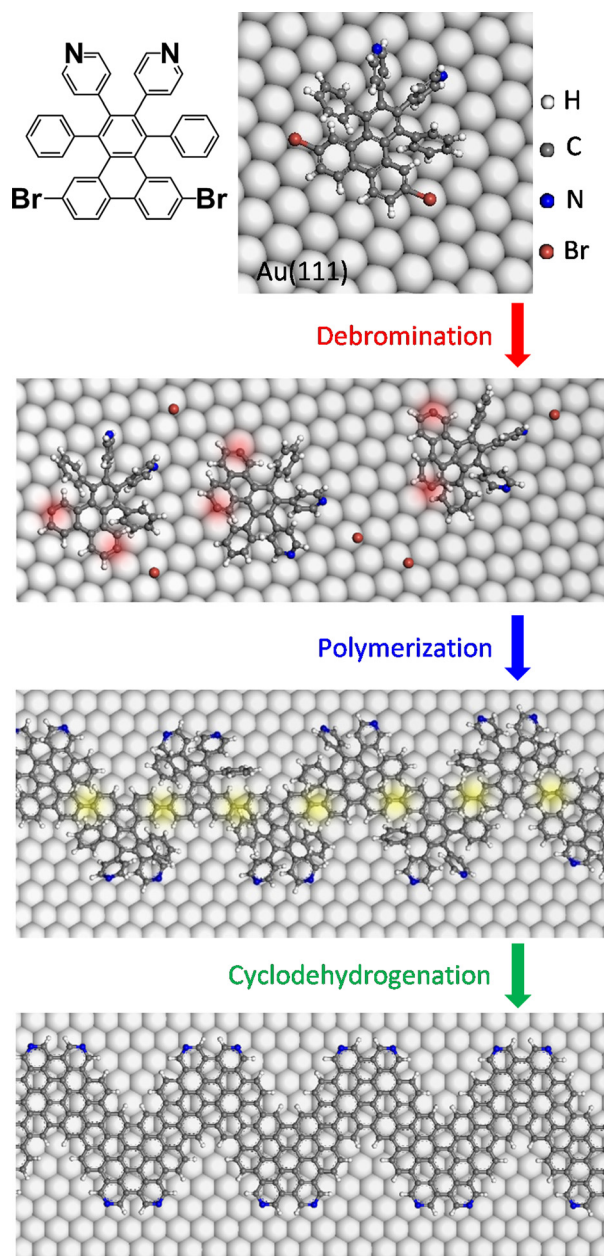


FIG. 1. Reaction scheme from the monomers to nitrogen-doped chevron-type GNRs. The monomers are thermally evaporated onto Au(111) and then undergo the debromination-polymerization process at 250 °C, forming the polymer chains. Further annealing to 450 °C, the cyclodehydrogenation process takes place and the NCGNRs form on the surfaces.

precursor monomer. Two nitrogen atoms are chemically introduced onto the monomer at particular positions which can serve as dopants for the resulting GNRs. After depositing the monomers onto Au(111), the GNRs are obtained via a two-step annealing process: debromination-polymerization and intramolecular cyclodehydrogenation, which take place at 250 °C and 450 °C, respectively. When the annealing temperature reaches 250 °C, the biradical monomers, resulting from the cleavage of the C-Br bonds, polymerize with each other and form polyphenylene precursors. By further annealing the sample at 450 °C, the polymers undergo the surface-assisted cyclodehydrogenation process and form the final product.

First, we studied the adsorption behavior of the monomers before thermal annealing and found that they grew along the herringbone reconstruction at sub-monolayer coverage, as shown in the large area STM image [Fig. 2(a)]. A zoom-in image of the green square area in Fig. 2(a) clearly shows that the monomers preferentially occupy the fcc regions, leaving the hcp regions totally unoccupied [Fig. 2(b)]. This kind of preferential adsorption phenomenon commonly exist in molecules adsorbed on Au(111) due to the higher adsorption energy on the fcc region than the hcp region and ridges.^{28–30} Fig. 2(c) shows a high-resolution STM image of the monomers. The monomers adopt a non-coplanar configuration, in which each of the pyridyl rings and the phenyl groups rotates a certain angle around the single C-C bond due to the intramolecular H-H repulsion²¹ and appears as a bright spot in the STM image. These non-coplanar groups significantly contribute to the electronic states observed by the STM, while the bromo-substituted phenyl rings keep planar with the Au(111) surface and therefore can be hardly distinguished in the STM image.¹⁰

After annealing the sample at 450 °C for 30 min, the NCGNRs were formed via the intramolecular cyclodehydrogenation of polyphenylene precursors [Fig. 3(a)]. At first glance, we notice that the NCGNRs no longer grow along the herringbone reconstruction of Au(111) as the monomers do without annealing process. This is significantly different from the non-doped chevron-type GNRs fabricated by the similar precursor monomers without nitrogen components.¹⁰

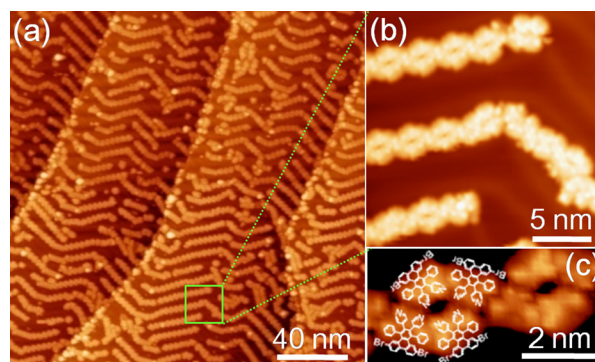


FIG. 2. Self-assembly of the monomers on Au(111). (a) Large area STM image before the annealing process. The molecules grow along the herringbone structure of Au(111). (b) Zoom-in STM image obtained from the green square area indicates that the molecules preferentially occupy the fcc regions of Au(111). (c) High resolution STM image of the molecular chains. Four configurations are superimposed to guide the eyes. Scanning parameters: $V_s = -3.0$ V, $I_t = 50$ pA for all three images.

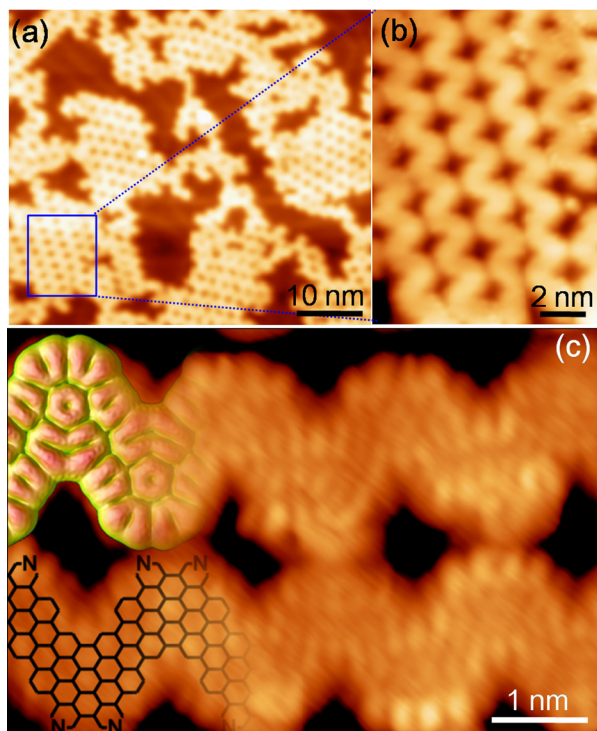


FIG. 3. STM images of the NCGNRs. (a) STM image after annealing the sample to 450 °C. The NCGNRs aligned side by side with different orientation domains. (b) Zoom-in STM image. (c) High resolution STM image of the NCGNRs with a DFT-based STM simulation model and a formula structure superimposed. Scanning parameters: $V_s = -3.0$ V, $I_t = 50$ pA for (a); $V_s = -1.0$ V, $I_t = 50$ pA for (b); and $V_s = -2.0$ V, $I_t = 0.10$ nA for (c).

Taking a close look at Fig. 3(a), we further recognized that the NCGNRs formed several domains with different orientation with respect to the substrate. They self-organized into arrays and laid alongside their neighbors within each domain. Fig. 3(b) is a zoom-in image obtained from the blue square area in Fig. 3(a) and gives more details about the ribbons. One important result is that the ribbons adopt a rigorous side by side arrangement, with the vertexes of the chevron-shape against to each other. Moreover, the ribbon interval is uniform and estimated to be just a few angstroms. It should be noticed that the NCGNRs, with a periodicity of 1.80 nm, have a pure armchair edge structure which is predetermined by the precursor we used and the widths alternate between $N=6$ and $N=9$. The particular structure of the NCGNRs requires that the orientation of the adjacent monomers should be reversed with respect to each other. Therefore, the pairs of nitrogen incorporation alternatively distribute at the two sides of the ribbons. Fig. 3(c) shows a high-resolution STM image of the NCGNRs, with a DFT-based STM simulation model and a formula structure superimposed. The agreement between them further confirms that we have fabricated the GNRs with atomically precise nitrogen doping and pure armchair edges.

Since the local electronic structure is a crucial feature of the GNRs, we then performed STS measurements on the as-prepared samples with sub-monolayer coverage of NCGNRs. The STS measurements were carried out in constant tip height mode, using the lock-in technique with a $V_{rms} = 17$ mV sinusoidal modulation signal at 773 Hz. Positive bias voltages correspond to tunneling of electrons from the tip to unoccupied

states in the sample. dI/dV curves on the bare Au(111) surface were recorded for many times before and after we measured the corresponding curves on NCGNRs to make sure that the tip was in good condition. Fig. 4(a) shows the averaged STS results recorded on NCGNRs (red curve) and bare Au(111) surface (black curve). The spectrum of NCGNRs has been vertically offset for clarity. The dI/dV curve obtained on the bare Au(111) surface exhibits the characteristic Shockley surface state with a peak at -0.47 eV. As for the curve obtained on the NCGNRs, two significant peaks are observed: one is centered at -0.39 eV and the other is centered at 0.63 eV. We interpret them as the valence band maximum (VBM) and conduction band minimum (CBM), respectively. Thus, the band gap of the NCGNRs can be derived from these two peaks with a value of $E_g = 1.02 \pm 0.05$ eV. A small shoulder located at -0.5 eV is also observed as indicated by the black arrow, and we attribute it to the Shockley surface state of the Au(111) substrate. DFT calculations were also carried out to explore the electronic structure of the NCGNRs [Fig. 4(b)]. At the Γ point, the CBM and VBM are found to locate at $(E_f + 0.96)$ eV and $(E_f - 0.23)$ eV, respectively. Therefore, the calculated band gap is 1.19 eV, which agrees well with the experiment result.

The NCGNRs demonstrated here are all fabricated under the circumstance of sub-monolayer precursor monomers. To further explore whether the coverage is an important factor for the growth of high-quality NCGNRs, controlled experiments with monolayer monomers were carried out. Interestingly, before the annealing process, the monolayer molecules adsorbed on Au(111) display unique orientation [Fig. 5(a)], with the main axis (marked by solid blue arrow) of each single molecule roughly parallel to the $[11\bar{2}]$ direction of Au(111) surface but rotated by about 12° from the molecular lattice vector (marked by dotted yellow arrow). This feature persists in all of our samples with monolayer coverage. A higher resolution STM image is shown as inset of Fig. 5(a) and every single molecule can be clearly distinguished. A structural formula of the monomer as well as its main axis (solid blue arrow) is also superimposed to guide the eyes. After annealing the sample at 450 °C for 30 min, the so-called graphene nanoribbons

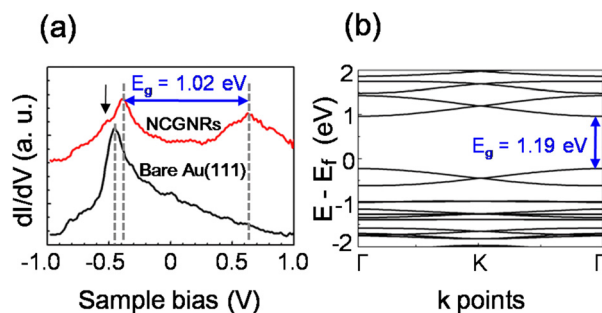


FIG. 4. Electronic structure of the NCGNRs. (a) Averaged dI/dV spectra obtained on bare Au(111) (black) and NCGNRs (red). The spectrum on NCGNRs has been offset vertically for clarity. An obvious Shockley surface state peak was observed at -0.47 eV, which confirmed the good condition of the tip. A gap of 1.02 eV was derived ($V_s = -1.0$ V, $I_t = 0.40$ nA, modulation voltage $V_{rms} = 10$ mV with the open-feed-back mode.). (b) DFT calculation result of the band structure of the NCGNRs. The CBM and VBM are located at $(E_f + 0.96)$ eV and $(E_f - 0.23)$ eV, respectively. The calculated band gap is 1.19 eV.

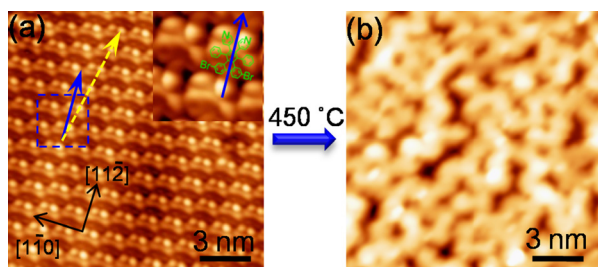


FIG. 5. STM images obtained from the controlled experiments with high coverage monomers. (a) STM image of monolayer molecules adsorbed on Au(111) before the annealing process. The molecules adopt a unique orientation and close-packed on Au(111). The solid blue arrow and dotted yellow arrow indicate the main axis of the monomer and the molecular lattice vector, respectively. Inset shows the high resolution STM image in which every single molecule can be identified. (b) STM image of the short and disordered ribbons after annealing the sample to 450 °C. Scanning parameters: $V_s = -2.0$ V, $I_t = 0.10$ nA for both (a) and the inset; $V_s = -3.0$ V, $I_t = 50$ pA for (b).

formed on the Au(111) surface, but all the ribbons are very short and the alignment is disordered [Fig. 5(b)], which is significantly different from our previous results with sub-monolayer coverage. This result can be easily understood if we take a close look into the structure of NCGNRs. As we have mentioned previously, every monomer has to rotate an 180° angle with respect to its two nearest neighbors to form the precursor polymers. In the case of monolayer coverage, the monomers arrange in the same orientation, and the space between each other is very limited. During the annealing process, each monomer can only be coupled with its nearest neighbors, since diffusion and rotation are both restricted by the high coverage. The special requirement on the orientation of the monomers to form NCGNRs, together with the unique orientation of the monomers at high coverage, give rise to the short and disordered NCGNRs. In fact, most of them are just dimers, trimers, and tetramers, which may not be called as nanoribbons by definition, due to the rather low aspect ratios. We thus conclude that high quality NCGNRs can only be fabricated with sub-monolayer coverage.

In conclusion, we have synthesized the atomically precise nitrogen-doped chevron-type graphene nanoribbons by selective nitrogen substitution of the precursor monomers. STM experiments and DFT calculations indicate a band gap around 1 eV. Compared with the similar chevron-type GNRs without nitrogen doping, our results show that atomically precise bottom-up nitrogen doping is an efficient way to tune the band gaps of the GNRs. This work highlights that other nitrogen-doped GNRs with different numbers of nitrogen atoms and different doping sites could be fabricated via this way.

This work was financially supported by the NSFC (Nos. 51325204, 61390501 and 51210003) and MOST (Nos. 2011CB932700 and 2011CB921702) of China.

- ¹K. Wakabayashi, M. Fujita, H. Ajiki, and M. Sigrist, *Phys. Rev. B* **59**, 8271–8282 (1999).
- ²K. Kusakabe and M. Maruyama, *Phys. Rev. B* **67**, 092406 (2003).
- ³Y. W. Son, M. L. Cohen, and S. G. Louie, *Nature* **444**, 347–349 (2006).
- ⁴V. Barone, O. Hod, and G. E. Scuseria, *Nano Lett* **6**, 2748–2754 (2006).
- ⁵Y.-W. Son, M. L. Cohen, and S. G. Louie, *Phys. Rev. Lett.* **97**, 216803 (2006).
- ⁶M. Han, B. Özyilmaz, Y. Zhang, and P. Kim, *Phys. Rev. Lett.* **98**, 206805 (2007).
- ⁷L. Yang, C.-H. Park, Y.-W. Son, M. Cohen, and S. Louie, *Phys. Rev. Lett.* **99**, 186801 (2007).
- ⁸X. L. Li, X. R. Wang, L. Zhang, S. W. Lee, and H. J. Dai, *Science* **319**, 1229–1232 (2008).
- ⁹L. Y. Jiao, L. Zhang, X. R. Wang, G. Diankov, and H. J. Dai, *Nature* **458**, 877–880 (2009).
- ¹⁰J. Cai, P. Ruffieux, R. Jaafar, M. Bieri, T. Braun, S. Blankenburg, M. Muoth, A. P. Seitsonen, M. Saleh, X. Feng, K. Mullen, and R. Fasel, *Nature* **466**, 470–473 (2010).
- ¹¹H. Huang, D. Wei, J. Sun, S. L. Wong, Y. P. Feng, A. H. Neto, and A. T. Wee, *Sci. Rep.* **2**, 983 (2012).
- ¹²Y. C. Chen, D. G. de Oteyza, Z. Pedramrazi, C. Chen, F. R. Fischer, and M. F. Crommie, *ACS Nano* **7**, 6123–6128 (2013).
- ¹³H. Zhou, J. Liu, S. Du, L. Zhang, G. Li, Y. Zhang, B. Z. Tang, and H. J. Gao, *J. Am. Chem. Soc.* **136**, 5567–5570 (2014).
- ¹⁴L. Grill, M. Dyer, L. Lafferentz, M. Persson, M. V. Peters, and S. Hecht, *Nat. Nanotechnol.* **2**, 687–691 (2007).
- ¹⁵H. J. Gao and L. Gao, *Prog. Surf. Sci.* **85**, 28–91 (2010).
- ¹⁶P. Ruffieux, J. M. Cai, N. C. Plumb, L. Patthey, D. Prezzi, A. Ferretti, E. Molinari, X. L. Feng, K. Mullen, C. A. Pignedoli, and R. Fasel, *ACS Nano* **6**, 6930–6935 (2012).
- ¹⁷B. Huang, Q. Yan, G. Zhou, J. Wu, B.-L. Gu, W. Duan, and F. Liu, *Appl. Phys. Lett.* **91**, 253122 (2007).
- ¹⁸N. Gorjizadeh, A. Farajian, K. Esfarjani, and Y. Kawazoe, *Phys. Rev. B* **78**, 155427 (2008).
- ¹⁹S. Dutta, A. K. Manna, and S. K. Pati, *Phys. Rev. Lett.* **102**, 096601 (2009).
- ²⁰Y. F. Li, Z. Zhou, P. W. Shen, and Z. F. Chen, *ACS Nano* **3**, 1952–1958 (2009).
- ²¹C. Bronner, S. Stremlau, M. Gille, F. Braue, A. Haase, S. Hecht, and P. Tegeder, *Angew. Chem. Int. Ed.* **52**, 4422–4425 (2013).
- ²²I. Horcas, R. Fernandez, J. M. Gomez-Rodriguez, J. Colchero, J. Gomez-Herrero, and A. M. Baro, *Rev. Sci. Instrum.* **78**, 2432410 (2007).
- ²³G. Kresse and J. Hafner, *Phys. Rev. B* **47**, 558–561 (1993).
- ²⁴G. Kresse and J. Furthmuller, *Comput. Mater. Sci.* **6**, 15–50 (1996).
- ²⁵J. P. Perdew, K. Burke, and M. Ernzerhof, *Phys. Rev. Lett.* **77**, 3865–3868 (1996).
- ²⁶P. E. Blochl, *Phys. Rev. B* **50**, 17953–17979 (1994).
- ²⁷J. Tersoff and D. R. Hamann, *Phys. Rev. B* **31**, 805–813 (1985).
- ²⁸P. Maksymovych, D. C. Sorescu, and J. T. Yates, *Phys. Rev. Lett.* **97**, 146103 (2006).
- ²⁹Z. H. Cheng, L. Gao, Z. T. Deng, N. Jiang, Q. Liu, D. X. Shi, S. X. Du, H. M. Guo, and H. J. Gao, *J. Phys. Chem. C* **111**, 9240–9244 (2007).
- ³⁰N. Jiang, Y. Y. Zhang, Q. Liu, Z. H. Cheng, Z. T. Deng, S. X. Du, H. J. Gao, M. J. Beck, and S. T. Pantelides, *Nano Lett.* **10**, 1184–1188 (2010).